World Scientific
www.worldscientific.com

Fabrication and photocatalytic performance of electrospun PVA/silk/TiO$_2$ nanocomposite textile

Ming-Chung Wu*, Shun-Hsiang Chan and Ting-Han Lin

Department of Chemical and Materials Engineering, College of Engineering
Chang Gung University, Guishan Dist., Taoyuan City 33302, Taiwan
*mingchungwu@mail.cgu.edu.tw

Many organic/inorganic nanocomposites have been fabricated into fibrous materials using electrospinning techniques, because electrospinning processes have many attractive advantages and the ability to produce relatively large-scale continuous films. In this study, the polyvinyl alcohol (PVA)/silk/titanium dioxide (TiO$_2$) nanocomposite self-cleaning textiles were successfully produced using electrospinning technique. After optimizing electrospinning conditions, we successfully obtained the PVA/silk/TiO$_2$ nanocomposite fibers with average diameter of ~220 nm and TiO$_2$ concentration can be as high as 18.0 wt.%. For the case of the PVA/silk/TiO$_2$ nanocomposite textile, the color of brilliant green coated on the textile surface changed from the initial green color to colorless after ultraviolet (UV) irradiation. Because of its worthy photocatalytic performance, the developed PVA/silk/TiO$_2$ nanocomposite materials in this study will be beneficial for the design and fabrication of multifunctional fibers and textiles.

Keywords: Electrospinning processes; TiO$_2$; photocatalyst; nanocomposite; textile.

Titanium dioxide (TiO$_2$) has been used to address several aspects of modern renewable energy production. These include efficient working electrodes of dye-sensitized solar cells,[1] the hole blocking layers of polymer solar cells,[2] hydrogen production by photocatalytic water splitting[3,4] and management of environmental pollution.[5] Until now, TiO$_2$ is still the subject of intensive research as the most promising photocatalyst because of good photocatalytic activity and excellent photostability. At the same time, it is environmentally friendly and low cost. Several studies have focused on the effect of TiO$_2$ to improve indoor and outdoor air quality and to treat waste water due to the significantly increased emission of volatile organic compounds (VOCs), coloring agents, and industrial dye wastes amongst others.[6,7] The ultraviolet (UV) radiation excited TiO$_2$ plays an important role in the degradation of VOCs and organic dyes. Photodegradation includes photodissociation, the breakup of VOCs and organic dyes into smaller pieces by photons.[8] Langmuir–Hinshelwood kinetic model may be the possible mechanism commonly used by TiO$_2$ to describe photocatalytic degradation kinetics.[9,10] Many literatures reported that fibrous materials can exhibit much better mechanical properties than the particles materials.[10,11] While using inorganic materials to fabricate flexible textile is still a challenge, many research groups

adopted organic/inorganic nanocomposites to produce flexible textile. Electrospinning technique is also used to prepared organic/inorganic nanocomposite fiber in the sub-micro and nanoscale, because of its applicability to various materials and the ability to generate relatively large-scale continuous films.[12–18] Doshi and Reneker reported the principles of electrospinning technique in 1995.[19] The precursor solution for electrospinning process, which is held by its surface tension at the end of a capillary tube, is subject to an electric field. Charge is induced on the precursor solution surface by the high voltage electric field. Similar charge repulsion causes a force directly opposite to the surface tension. As the intensity of the electric field is increased, the hemispherical surface of the solution at the tip of the capillary tube elongates to form a conical shape known as the Taylor cone. When the electric field reaches a critical value at which the repulsive electric force overcomes the surface tension force, a charged jet of the solution is ejected from the tip of the Taylor cone. This trajectory can be controlled by an electric field because the jet is charged. As the jet travels in the air, the solvent evaporates. It leaves a charged polymer fiber, which lies randomly on a collecting metal screen.[19–22] For the organic part, polymer material plays an important role in fabricating textile. In this study, silk and polyvinyl alcohol (PVA) are chosen to prepare the organic/inorganic nanocomposites. Silk is one of the natural protein fibers which can be woven into strong and

---

*Corresponding author.

luxurious textiles. It has attracted significant attention in the development of new fiber materials due to its biodegradable and biocompatible characteristics, high chemical reactivity, and excellent mechanical properties.[23,24] For PVA, it is a highly biocompatible and non-toxic polymer. It can be processed easily and has high water permeability. PVA has extensive applications in air filtration, textile industry, and paper coating due to its flexibility and good chemical and thermal stability.[21,25]

Here, we developed a composite solution, consisted of PVA, silk and TiO_2 nanoparticles, to fabricate the nanocomposite fibers into flexible textiles using electrospinning technique. The nanocomposite fibers and flexible textiles were obtained successfully, after optimizing the parameters of electrospinning process. The photocatalytic performance of PVA/silk/TiO_2 nanocomposite flexible textile was also tested by measuring the photodegradation of organic dye. To our best knowledge, this maybe the first study to fabricate PVA/silk/TiO_2 nanocomposite fibers and textiles with self-cleaning properties.[26–29] Besides, PVA/silk/TiO_2 nanocomposite textile will be a good candidate material for the application of curtain textile.

In the experimental section, TiO_2 nanoparticles (Aeroxide™ P25, ACROS Organics) and PVA (MW~16,000 Da, Acros, 98%) were used as received without further purification. Silk fibroin was obtained from Bombyx mori silk cocoons that were degummed in a 0.5% (w/v) Na_2CO_3 (Fisher, 99.5%) at 95°C for 30 min. After thoroughly washing with warm water, silk fibroin was dried at room temperature. Silk fibroin solution was obtained from 10 mg of silk fibroin dissolved in 990 mg of bleach (Bailan, Unilever) with continuous stirring for 30 min. Silk fibroin solution was added to 1740 mg of a stirred of solution of distilled water prior to the 900 mg of PVA. Then, 100 mg, 200 mg and 400 mg of TiO_2 nanoparticle was added to silk/PVA solutions respectively. The final solutions were stirred for 40 min and degased by ultrasonic agitation. The compositions of various precursor solutions are shown in Table 1.

The electrospinning system includes the high-voltage power supply (HVPS, You-Shang Technical Corporation), the syringe pump (KDS100, KD Scientific Inc.), and the metallic collector. The maximum voltage of the high-voltage

Table 1. The compositions of various precursor solutions in this study.

Precursor solution	PVA (mg)	Silk (mg)	TiO_2 NPs (mg)
A	900	0	0
B	900	10	0
C	900	10	100
D	900	10	200
E	900	10	400

power supply is 40.0 kV with the minimum control resolution of 1.0 V. The syringe pump can precisely control the flow rates and volumes. It has the capacity to handle various-sized syringes. The rotational speed of the metallic collector can be tuned precisely. During the electrospinning process, the constant flow rate was fixed at 0.5 mL/h, and the tip-to-collector distance and applied high-voltage were fixed at 10.0 cm and 25 kV. The rotational speed of the metallic collector was 100 rpm. The flowchart of electrospinning process is shown in Fig. S1 of supplementary information.

The microstructures of various PVA/silk/TiO_2 nanocomposite fibers were observed by scanning electron microscopy (SEM, SNE-4500M, SEC Co. Ltd., Korea) operated at an accelerating voltage of 30.0 kV. The crystalline structures of various nanocomposite fibers were characterized by using X-ray diffraction (XRD, D5005, Siemens, Germany). Infrared spectra were measured by Fourier transform infrared spectroscopy (FTIR, Bruker Tensor-27 instrument, Germany). Potassium bromide pellets containing 1.0% of the samples were used in FTIR experiments and 32 scans were accumulated for each spectrum in transmission, at a spectral resolution of 2 cm^{-1}. To mimic decomposition of organic stains on the PVA/silk/TiO_2 nanocomposite flexible textile, a highlighter (Tombo, Coat II, WA-SC 93, Japan) was used to deposit dye on the flexible surface. Each sample was exposed to ultraviolet light (UV-B, G8T5E, 8 W, Sankyo Denki) for different lengths of time. The fading of the written pattern was recorded with a digital camera. Moreover, the samples were tested in the degradation of brilliant green, and they were irradiated with UV-B lamps. The absorption spectra of the retained brilliant green on the two textiles were recorded using an absorption spectrophotometer (JASCO Analytical Instruments, V-630, Japan) in the 450–900 nm wavelength range.

Different nanofiber morphologies can be obtained via control of the processing conditions. The SEM images of five samples (samples A, B, C, D and E) are shown in Fig. 1. Sample A is made by pristine PVA solution as shown in Fig. 1(a), and the SEM image shows no formation of fibrous materials for this solution with 25 wt.% PVA. Figure 1(b) shows sample B prepared by PVA/silk precursor solution. We can observe the PVA/silk blend fibers with diameters of ~380 nm on the aluminum foil substrate. The SEM images for the samples (samples C, D and E) made of PVA/silk/TiO_2 nanocomposite solutions with different TiO_2 concentration are shown in Figs. 1(c)–1(e). The diameters of nanocomposite fibers for samples C and D are 260 nm and 220 nm, respectively. However, the fibrous materials did not occurred for sample E (Fig. 1(e)), when the TiO_2 amount is at 400 mg for the PVA/silk/TiO_2 precursor solution. The diameter
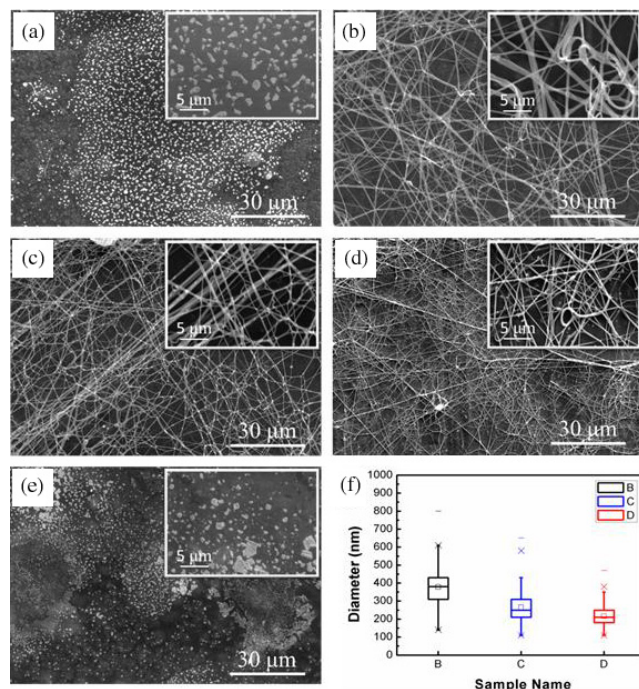
Fig. 1. SEM images of the results made by different precursor solution using electrospinning process, (a) sample A, (b) sample B, (c) sample C, (d) sample D, (e) sample E and (f) diameter distribution of the fibrous materials.

Fig. 3. FTIR spectra of TiO$_2$-P25, silk fibroin, PVA (sample A), PVA/silk (sample B) and PVA/silk/TiO$_2$ (sample D) in the wavenumber range of 3800–400 cm^{-1}.

distribution of samples B, C and D are shown in Fig. 1(f). The diameters of PVA/silk/TiO$_2$ nanocomposite fibers decreased with increasing the TiO$_2$ concentration. It may be caused by TiO$_2$ aggregation in the syringe needle.

From XRD patterns as shown in Fig. 2, we can observe the diffraction peaks come from the contributions of PVA, silk, and TiO$_2$. Sample B is only the PVA/silk textile, but samples C and D are the PVA/silk/TiO$_2$ textiles with different TiO$_2$ concentration. For samples C and D, all peaks can be perfectly indexed as the body-centered tetragonal lattice structure [JCPDS No. 89-4921] of anatase TiO$_2$. Moreover, the (110) reflection at 2θ of $\sim 27.2°$ comes from rutile TiO$_2$. The results are due to the TiO$_2$ nanoparticles (Aeroxide^{TM}

P25) incorporated into the textiles consisting of anatase phase and rutile phase.

FTIR spectra of various films in the wave number range of 3800–400 cm^{-1} were measured as shown in Fig. 3. The characteristic infrared absorption frequencies of PVA, silk fibroin and TiO$_2$-P25 are listed in Table S1 of supplementary information. The absorption band of TiO$_2$-P25 is in the range of 400–600 cm^{-1}, contributing to the vibrations of Ti–O. The two broad peaks at 1640 cm^{-1} and 3420 cm^{-1} which can be attributed to the surface-adsorbed water and hydroxyl groups were observed.[37] The absorption peaks of silk fibroin at 1650 cm^{-1} and 1511 cm^{-1} are amide I and amide II (N–H), while the amide III (C–N) of fibroin is at 1228 cm^{-1}. The main absorption peaks of the PVA are at 3446 cm^{-1} (OH group), 2940 cm^{-1} (C–H aliphatic) and 1722 cm^{-1} (C=O stretching). For FTIR spectra of PVA/silk film (sample B), we observed the representative bands as follows: OH group (3400–3600 cm^{-1}) for PVA and amide I (1600–1700 cm^{-1}) for silk fibroin in PVA/silk film. In addition, all the absorption peaks of PVA/silk film (sample B) and Ti–O vibration (400–600 cm^{-1}) of TiO$_2$ were also observed in PVA/silk/ TiO$_2$ film (sample D). The FTIR spectra revealed the chemical compositions of various samples, and are consistent with XRD study.

In this study, we used PVA/silk blend solutions with/ without TiO$_2$ photocatalysts to prepare the flexible textiles that enable easy handling. Using these textiles, we demonstrated photodegradation of the dye deposited on the textile surface as shown in Fig. 4. A letter "A" was written on the flexible textile, and then the textile were exposed to UV light for different lengths of time. Sample B consisting of PVA and silk showed only minor changes in the intensity of the color pattern. However, sample D, consisting of PVA, silk and TiO$_2$ nanoparticles, was able to degrade the deposited ink considerably. In the case of the PVA/silk/TiO$_2$ nanocomposite textile (sample D), the original stain was faded considerably after UV exposure of 8 h.
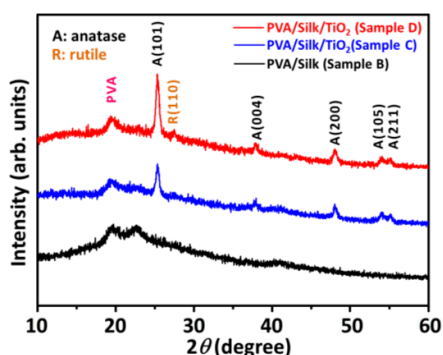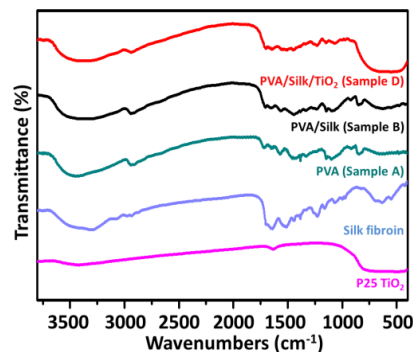

Fig. 2. XRD patterns of PVA/silk textile (sample B) and PVA/silk/TiO$_2$ textiles with different TiO$_2$ concentration (samples C and D).
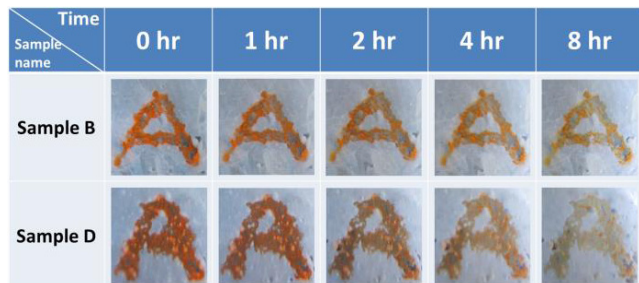
Fig. 4. Photographs of two textiles, sample B (PVA/silk textile) and sample D (PVA/silk/TiO$_2$ textile), showing the photodegradation of the dye deposited on the surface with different UV exposure time.

For the photodegradation activity test of samples B and D, we recorded the absorption spectra of brilliant green as a function of UV-B light irradiation time. Then, the absorbance measured at $\lambda = 660$ nm was used to calculate the amount of brilliant green using a calibration curve measured previously. The activities of two samples over the photodegradation of brilliant green under UV irradiation were measured and the results are shown in Fig. 5. The color of brilliant green coated on sample D changed from the initial green color to colorless after UV irradiation. In addition, the developed PVA/silk/TiO$_2$ nanocomposite materials will be beneficial for the design and fabrication of curtain with the multifunction of self-cleaning, deodorization, anti-bacterium, etc., as shown in Fig. S2 of supplementary information.

A technique for the manufacture of multifunctional PVA/silk/TiO$_2$ nanocomposite textile is successfully developed by using electrospinning process. The diameter of optimal PVA/silk/TiO$_2$ nanocomposite fibers can reach $\sim$220 nm, and its TiO$_2$ concentration is higher than 18.0 wt.%. For PVA/silk/TiO$_2$ nanocomposite textile, the color of brilliant green that on the textile surface changed from the initial green color
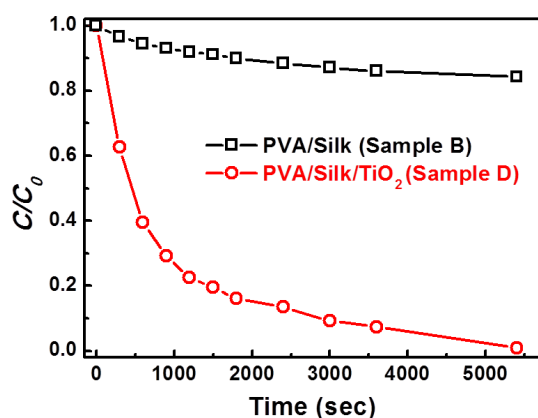
to colorless after UV irradiation of 1 h. Because of its notable photocatalytic performance, the developed PVA/silk/TiO$_2$ nanocomposite materials in this study will be beneficial for the design and fabrication of multifunctional fibers and textiles.

Acknowledgments

References

1. N. B. Gusiak *et al.*, *Funct. Mater. Lett.* **07**, 1450030 (2014).
2. M.-C. Wu *et al.*, *Nanoscale* **2**, 1448 (2010).
3. A. Kudo *et al.*, *Chem. Soc. Rev.* **38**, 253 (2009).
4. M. A. Fox *et al.*, *Chem. Rev.* **93**, 34 (1993).
5. M. R. Hoffmann *et al.*, *Chem. Rev.* **95**, 69 (1995).
6. H. Li *et al.*, *Funct. Mater. Lett.* **06**, 1330005 (2013).
7. Y. Wu *et al.*, *Appl. Catal. B* **88**, 525 (2009).
8. W. Sui *et al.*, *Funct. Mater. Lett.* **07**, 1350068 (2014).
9. A. Katti *et al.*, *Catal. Commun.* **10**, 2036 (2010).
10. M.-C. Wu *et al.*, *Nano Res.* **4**, 360 (2011).
11. W. Dong *et al.*, *J. Phys. Chem. B* **110**, 16819 (2006).
12. Z. M. Huang *et al.*, *Compos. Sci. Technol.* **63**, 2223 (2003).
13. N. M. Bedford *et al.*, *Adv. Energy Mater.* **2**, 1136 (2012).
14. S. J. Seo *et al.*, *Electrochem. Commun.* **13**, 1391 (2011).
15. W. H. Jung *et al.*, *Appl. Surf. Sci.* **261**, 343 (2012).
16. S. Ji *et al.*, *Sensor Actuat. B* **133**, 644 (2008).
17. B. Ding *et al.*, *Sensors-Basel.* **9**, 1609 (2009).
18. B. Ding *et al.*, *Mater. Today.* **13**, 16 (2010).
19. J. Doshi *et al.*, *J. Electrostat.* **35**, 151 (1995).
20. G. I. Taylor, *Jets. Proc. R. Soc. London A* **313**, 453 (1969).
21. M. S. Islam and M. R. Karim, *Colloid. Surface A* **366**, 135 (2010).
22. A. L. Yarin *et al.*, *J. Appl. Phys.* **90**, 4836 (2001).
23. H. Liu *et al.*, *Biomaterials* **32**, 3784 (2011).
24. Y. Kishimoto *et al.*, *Int. J. Biol. Macromol.* **57**, 124 (2013).
25. A. Koski *et al.*, *Mater. Lett.* **58**, 493 (2004).
26. G. Li *et al.*, *J. Colloid. Interf. Sci.* **358**, 307 (2011).
27. N. T. B. Linh *et al.*, *J. Mater. Sci.* **46**, 5615 (2011).
28. D. Y. Choi *et al.*, *Mater. Lett.* **106**, 41 (2013).
29. F. Li *et al.*, *Appl. Surf. Sci.* **276**, 390 (2013).
30. G. A. Koohmareh *et al.*, *Int. J. Polym. Sci.* **2011**, 190349 (2011).
31. S. Ling *et al.*, *Polym. Chem.* **4**, 5401 (2013).
32. H. S. Costa *et al.*, *J. Mater. Sci.* **43**, 494 (2008).
33. A. Pawlak and A. Mucha *et al.*, *Thermochim. Acta* **396**, 153 (2003).
34. Y. J. Lee *et al.*, *J. Appl. Polym. Sci.* **106**, 1337 (2007).
35. L. Niu *et al.*, *J. Nanomater.* **2010**, 729457 (2010).
36. J. Wang *et al.*, *J. Mater. Chem.* **19**, 6597 (2009).
37. T. Suprabha *et al.*, *Nanoscale Res. Lett.* **4**, 144 (2008).

Fig. 5. The photodegradation activity curves of two textiles over the photodegradation of brilliant green under UV irradiation.